Received: 11 September 2018 | Revised: 5 November 2018 | Accepted: 26 November 2018
DOI: 10.1002/aoc.4773

FULL PAPER

WILEY Applied Organometallic Chemistry

Fe_3O_4@SiO_2@Im-bisethylFc [HC_2O_4] as a novel recyclable heterogeneous nanocatalyst for synthesis of bis-coumarin derivatives

Reza Teimuri-Mofrad | Shabnam Tahmasebi | Elmira Payami

Department of Organic and Biochemistry, Faculty of Chemistry, University of Tabriz, Tabriz, Iran

Correspondence
Reza Teimuri-Mofrad, Department of Organic and Biochemistry, Faculty of Chemistry, University of Tabriz, Tabriz, Iran.
Email: teymouri@tabrizu.ac.ir

Nanomagnetic bisethylferrocene-containing ionic liquid supported on silica-coated iron oxide (Fe_3O_4@SiO_2@Im-bisethylFc [HC_2O_4]) as a novel catalyst was designed and synthesized. The described catalyst was recycled and used without change in the time and efficiency of the condensation reaction. The Fourier transform-infrared spectroscopy (FT-IR), scanning electron microscopy images, X-ray diffraction patterns, energy-dispersive X-ray spectroscopy, transmission electron microscope and vibrating-sample magnetometer results confirmed the formation of Fe_3O_4@SiO_2@Im-bisethylFc [HC_2O_4] magnetic nanoparticle. The novel bis-coumarin derivatives were identified by ^{1}H-NMR, ^{13}C-NMR, FT-IR and CHNS analysis.

KEYWORDS
4-hydroxycoumarin, bis-coumarin, ferrocene, ionic liquids, magnetic nanocatalyst

1 | INTRODUCTION

In recent years, heterogeneous catalysts based on ionic liquids (ILs) have become very important because magnetic nanoparticles (MNPs)-supported catalysts are a bridge between homogeneous and heterogeneous catalysts,[1,2] and those MNPs are suitable supports for ILs.[3] ILs also have received a great deal of attention as a catalyst in green organic synthesis because of their special characteristics, for example, high ionic conductivity, excellent chemical stability, no flammability, thermal and chemical stability, very low vapor pressure, selective solubility of water and organic solvents, recyclability and negligible volatility.[4–7] During the past few decades, ferrocene-based ligands have been widely studied due to their electron-rich aromatic structural motifs.[8] Ferrocene (Fc) and its derivatives are excellent and are often used in electrochemical systems as a protein biomarker or redox active species for detecting biomolecules, due to the reversibility, regeneration at low potential, and generation of stable redox states.[9] In addition, they are relatively low cost, thermal stability, high tolerance to moisture and oxygen, and have very unique chemical properties that make these materials attractive.[8] MNPs have attracted considerable interest due to magnetic and electrical properties, their extremely catalytic activity and the high surface to volume ratio, the wide range of applications in drug delivery systems, targeted gene therapy, ion exchange separation, magnetic resonance imaging, biosensors, magnetic data storage, and environmental remediation and catalysis.[10] The combination of the magnetic properties of Fe_3O_4 and SiO_2 shell and modification of this with ferrocene, give a stable, well-defined electrochemical signal, simplified procedure and accelerate the determination of pathogens in biological objects.[11]

4-Hydroxycoumarin has become very popular due to its special properties, as well as its many biological uses, and this has led to the synthesis and identification of various derivatives of bis-coumarin. These derivatives have been found useful in an extensive range of biological and pharmaceutical actions, including enzyme inhibitors,[12,13] anticoagulants,[14,15] antioxidants,[16,17] antitumor drugs,[18] anti-diabetic (α-glucosidase inhibitors) [19] urease inhibitors,[20,21] anticancers,[22] antibacterials,[23] inhibit c-Met phosphorylation in BaF_3/TPR-Met and EBC-1 NSCLC cell lines,[24] antimicrobial,[25] antiviral,[26] proliferation inhibition of K-562[27] and inhibit HIV-1.[28] Recently, several methods have been reported for the synthesis of bis-coumarin by the reaction of 4-hydroxycoumarin and various aldehydes in the presence of various homogeneous and heterogeneous catalysts and under various reaction conditions, such as tetrabutylammonium bromide (TBAB),[29] molecular iodine,[30] [bmin] BF_4,[31] SO_3H-functionalized IL,[32] sodium dodecyl sulfate,[33] piperidine,[34] n-dodecylbenzene sulfonic acid (DBSA),[35] [pyridin-SO_3H] Cl,[36] TrBr and [$Fe_3O_4@SiO_2@(CH_2)_3$-Im-SO_3H]Cl,[37] MNPs-PSA[38] and $Fe_3O_4@SiO_2@(CH_2)_3$semicarbazide-SO_3H/HCl.[39] Although all the procedures for the synthesis of corresponding bis-coumarin have their merits, the main disadvantages of these methods are often tedious work-up procedures, low yields, harsh reaction conditions, and the use of toxic, corrosive and expensive catalysts, and the recovery of these catalysts are often difficult.

Herein, in continuation of previous research on the synthesis of ferrocene-IL-based MNPs for catalysis of multi component reactions,[40–44] in this work we report the synthesis and structural characterization of $Fe_3O_4@SiO_2@$Im-bisethylFc [HC_2O_4] as a novel recyclable heterogeneous nanocatalyst and also, using this new synthesized nanocatalyst, we were able to provide a simple and effective way of synthesizing bis-coumarin derivatives under reflux conditions in ethanol (Scheme 1).

2 | RESULTS AND DISCUSSION

2.1 | Preparation and characterization of $Fe_3O_4@SiO_2@$Im-bisethylFc [HC_2O_4] magnetic nanocatalyst

The synthesis process of magnetic nanocatalyst ($Fe_3O_4@SiO_2@$Im-bisethylFc [HC_2O_4]) is shown in Scheme 2. In the first step, Fe_3O_4 nanoparticles were prepared by a chemical co-precipitating method. Then, Fe_3O_4 nanoparticles with an outer layer of silica, which not only prevents aggregation of the nano-sized particles but also provides numerous surfaces for Si-OH groups for further modifications, were synthesized. The silica-coated MNPs were subsequently reacted with (3-chloropropyl)triethoxysilane.[45–47] Then, chlorine was replaced by imidazole on the modified nanoparticle surface.

In the second step, ethylferrocene was reacted with 5-chloropentan-2-one in the presence of sulfuric acid and methanol mixture, and 5-chloro-2,2-bis (ethylferrocenyl) pentane was obtained. Finally, bisethylferrocene-containing IL supported on MNPs was synthesized via the reaction of imidazolepropyl modified silica-coated MNPs with 5-chloro-2,2-bis (ethylferrocenyl) pentane to afford $Fe_3O_4@SiO_2@$Im-bisethylFc [Cl], afterwards the reaction between $Fe_3O_4@SiO_2@$Im-bisethylFc [Cl] and oxalic acid mono sodium salt resulted in the synthesis of the final magnetic nanocatalyst (Scheme 2).

The structure of $Fe_3O_4@SiO_2@$Im-bisethylFc [HC_2O_4] catalyst was studied and completely characterized using Fourier transform-infrared spectroscopy (FT-IR), field-emission-scanning electron microscopy (FE-SEM), energy-dispersive X-ray spectroscopy (EDX), X-ray diffraction (XRD), transmission electron microscopy (TEM) and vibrating-sample magnetometer (VSM) analysis.

SCHEME 1 The synthesis of bis-coumarin derivatives using $Fe_3O_4@SiO_2@$Im-bisethylFc [HC_2O_4] as an efficient catalyst

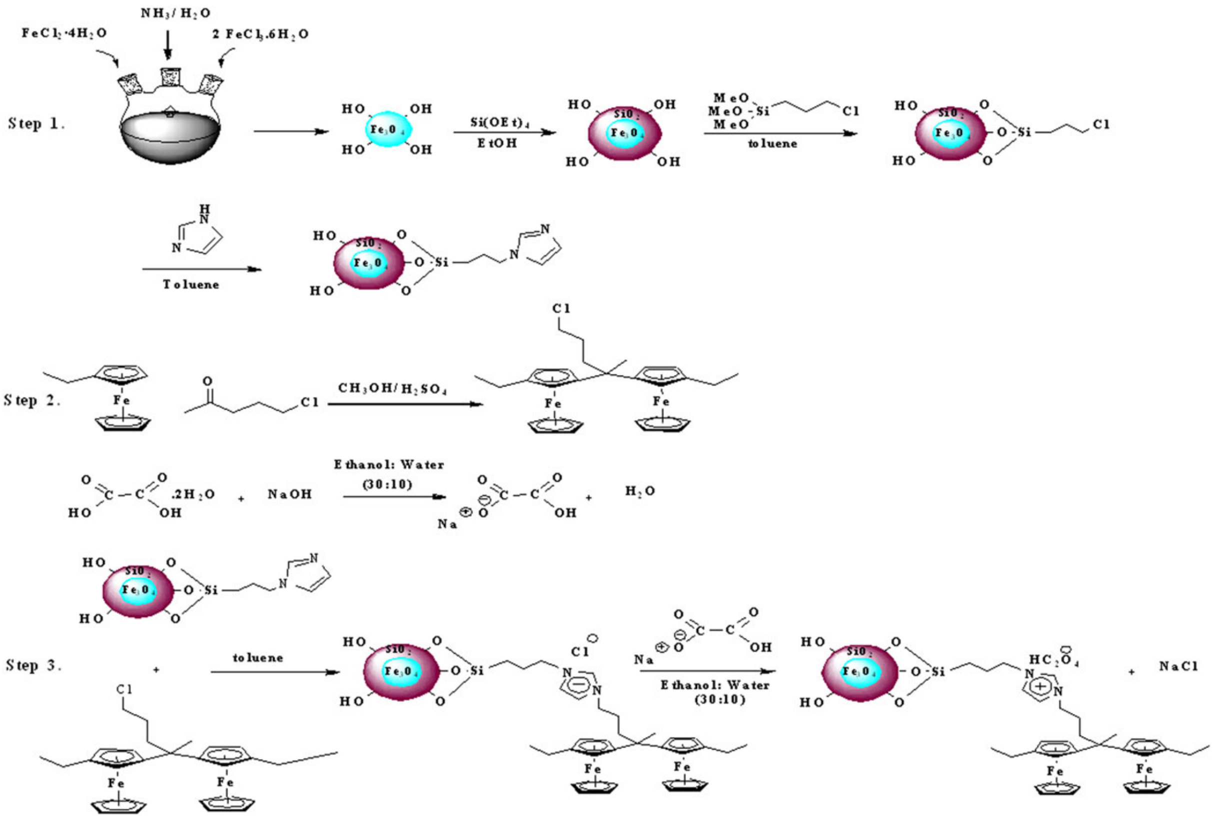

SCHEME 2 Synthesis of $Fe_3O_4@SiO_2@$Im-bisethylFc $[HC_2O_4]$ magnetic nanocatalyst

The corresponding FT-IR spectra of the MNPs: (a) Fe_3O_4, (b) $Fe_3O_4@SiO_2$, (c) $Fe_3O_4@SiO_2\text{-}(CH_2)_3Cl$, (d) $Fe_3O_4@SiO_2@$Im, (e) $Fe_3O_4@SiO_2@$Im-bisethylFc [Cl] and (f) $Fe_3O_4@SiO_2@$Im-bisethylFc $[HC_2O_4]$ are shown in Figure 1. In the FT-IR spectrum of the Fe_3O_4 (Figure 1a), the presence of two absorption peaks at about 584 cm^{-1} and 3434 cm^{-1} related to Fe-O bonds and hydroxyl groups present at the nanoparticle surface, respectively. The two absorption peaks observed at 802 cm^{-1} and 1088 cm^{-1} in the FT-IR spectrum of $Fe_3O_4@SiO_2$ MNPs (Figure 1b) are related to the Si-O-Si bond symmetric and asymmetric tensile vibrations, respectively. Also, the observed peak at about 465 cm^{-1} was assigned to the bending vibration of Si-O-Si bond. The observed absorption peak at 3445 cm^{-1} is also related to hydroxyl groups. The FT-IR spectrum of $Fe_3O_4@SiO_2\text{-}(CH_2)_3Cl$ (Figure 1c), in addition to having similar peaks in the two interpreted spectra above, has two peaks at 2849 cm^{-1} and 2918 cm^{-1}, which relate to the symmetric and asymmetric tensile vibrations in the carbon chain, respectively. In the FT-IR spectrum of $Fe_3O_4@SiO_2@$Im (Figure 1d), the appearance of new peaks at 1485 cm^{-1} and 1515 cm^{-1} relates to the tensile vibrations of C=C and C=N in the imidazole ring, respectively. Finally, the FT-IR spectra of $Fe_3O_4@SiO_2@$Im-bisethylFc $[HC_2O_4]$ MNPs (Figure 1f) show an absorption peak at about 1682 cm^{-1}, which was related to the vibration of the carbonyl bond, and the peak that appeared at 1089 cm^{-1} referred to the tensile vibration of the C-O bond of the anion.

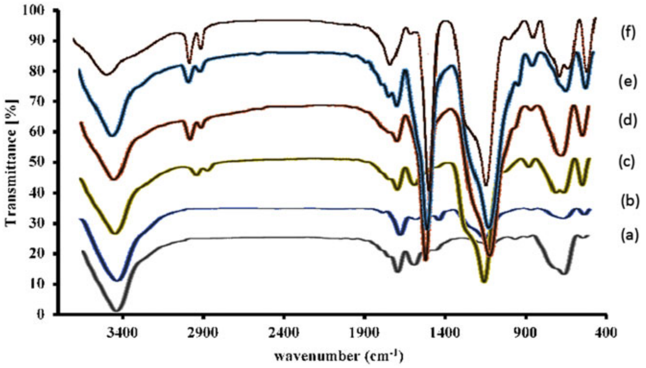

FIGURE 1 The Fourier transform-infrared (FT-IR) spectra of (a) Fe_3O_4, (b) $Fe_3O_4@SiO_2$, (c) $Fe_3O_4@SiO_2@(CH_2)_3Cl$, (d) $Fe_3O_4@SiO_2@$Im, (e) $Fe_3O_4@SiO_2@$Im-bisethylFc [Cl] and (f) $Fe_3O_4@SiO_2@$ Im-bisethylFc $[HC_2O_4]$

The surface morphology and particle size of: (a) $Fe_3O_4@SiO_2$, (b) $Fe_3O_4@SiO_2@$Im-bisethylFc [Cl] and (c) $Fe_3O_4@SiO_2@$Im-bisethylFc $[HC_2O_4]$ nanoparticles were studied by FE-SEM analysis, and the images are shown in Figure 2. Spherical morphology with an average

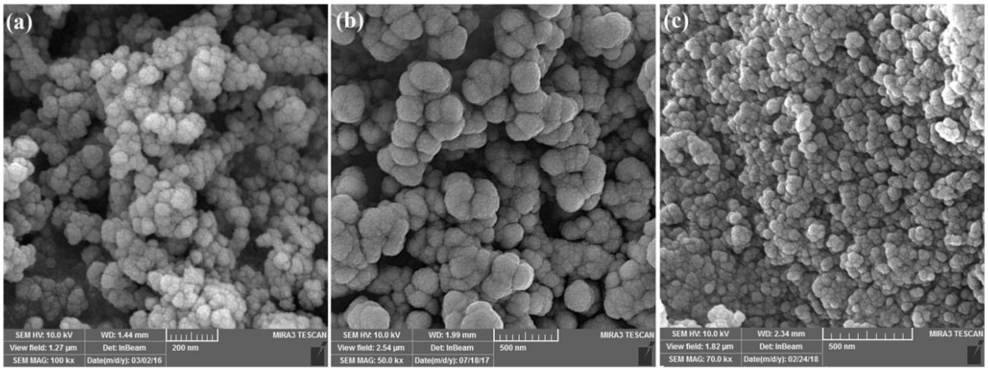

FIGURE 2 Field-emission-scanning electron microscopy (FE-SEM) images of (a) Fe$_3$O$_4$@SiO$_2$, (b) Fe$_3$O$_4$@SiO$_2$@Im-bisethylFc [Cl] and (c) Fe$_3$O$_4$@SiO$_2$@Im-bisethylFc [HC$_2$O$_4$]

diameter of about 20 nm for catalyst was observed. Also, according to the particle size distribution diagram of the final synthesized nanocatalyst Fe$_3$O$_4$@SiO$_2$@Im-

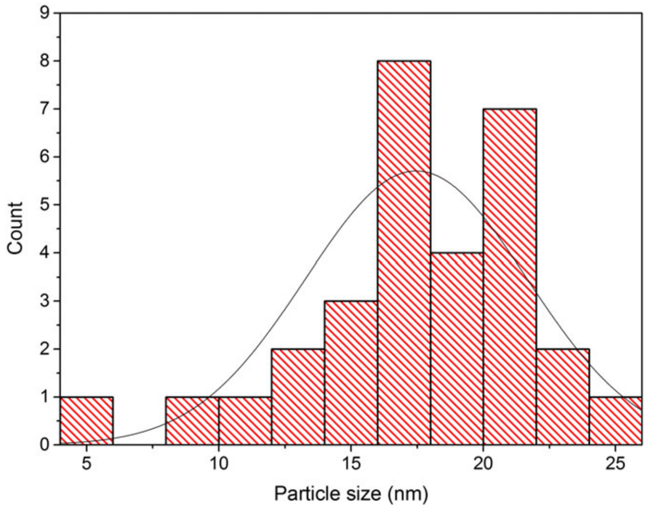

FIGURE 3 Particle size distribution diagram of Fe$_3$O$_4$@SiO$_2$@Im-bisethylFc [HC$_2$O$_4$]

TABLE 1 EDX analysis data for Fe$_3$O$_4$@SiO$_2$@Im-bisethylFc [HC$_2$O$_4$]

Element	C	N	O	Si	Fe	Total
Weight (%)	36.88	4.26	50.93	5.20	2.73	100.00

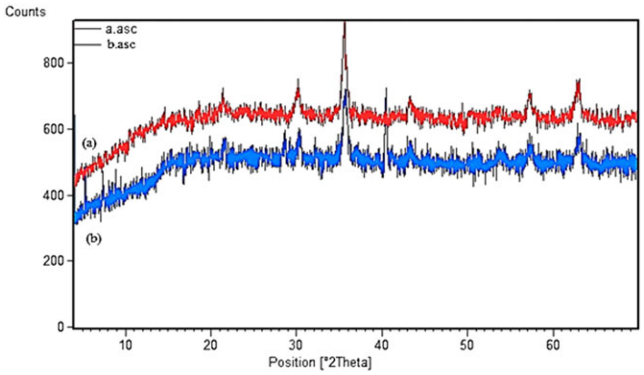

FIGURE 5 X-ray diffraction (XRD) patterns of (a) Fe$_3$O$_4$@SiO$_2$@Im-bisethylFc [Cl] and (b) Fe$_3$O$_4$@SiO$_2$@Im-bisethylFc [HC$_2$O$_4$]

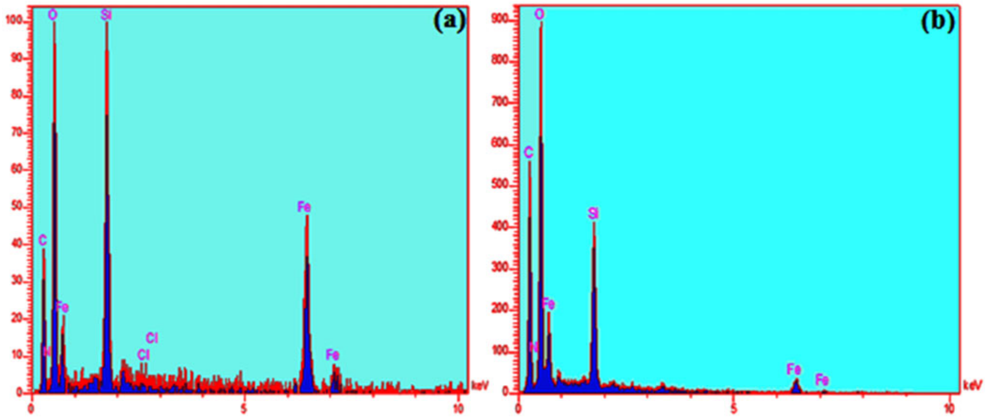

FIGURE 4 Energy-dispersive X-ray spectrometry (EDX) analysis of (a) Fe$_3$O$_4$@SiO$_2$@Im-bisethylFc [Cl] and (b) Fe$_3$O$_4$@SiO$_2$@Im-bisethylFc [HC$_2$O$_4$]

bisethylFc [HC_2O_4] as shown in Figure 3, the nanoparticle size of the final nanocatalyst is about 20 nm.

The EDX spectra of the novel synthesized nanocatalyst Fe_3O_4@SiO_2@Im-bisethylFc [HC_2O_4] are shown in Figure 4. Accordingly, the presence of the elements Fe, Cl, Si, O, N and C in the synthesized nanocatalyst is corroborated. The elements ratio of the Fe_3O_4@SiO_2@Im-bisethylFc [HC_2O_4] nanocatalyst was measured by EDX analysis, and data were collected in Table 1. It is noteworthy that there is no chlorine in the final nanocatalyst, which indicates the successful replacement of chlorine with oxalate in the final nanocatalyst.

The XRD patterns of the modified Fe_3O_4 nanoparticles are depicted in Figure 5. As can be noted from the spectra, the diffusion pattern of the modified Fe_3O_4 nanoparticles shows only the crystalline dispersions of the Fe_3O_4 MNPs. The presence of similar peaks in the spectra of Fe_3O_4@SiO_2@Im-bisethylFc [Cl] and Fe_3O_4@SiO_2@Im-bisethylFc [HC_2O_4] indicates that the crystalline structure of the nanoparticles is the same, and this proves that the crystalline structure of the nanoparticles remains unchanged during the steps of the surface modification.

Figure 6 shows the TEM image analysis. TEM images were used to estimate the particle size of Fe_3O_4@SiO_2@Im-bisethylFc [HC_2O_4], which was determined from the histogram data to be smaller than 40 nm. Also, from the resulting TEM image, we find that core-shell nanoparticles are formed.

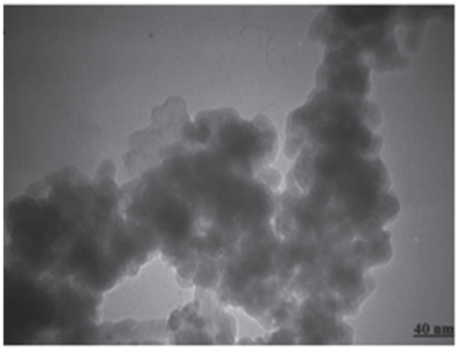

FIGURE 6 Transmission electron microscopy (TEM) image of Fe_3O_4@SiO_2@Im-bisethylFc [HC_2O_4]

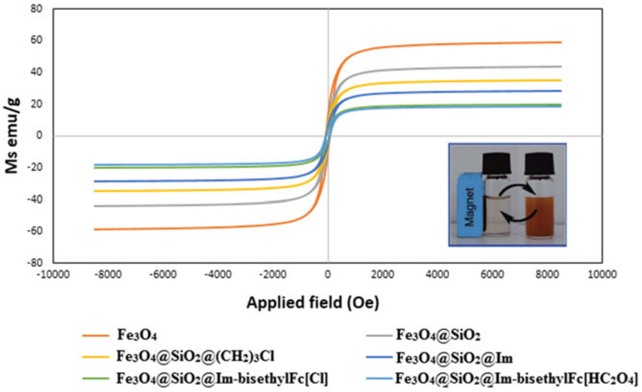

FIGURE 7 Vibrating-sample magnetometer (VSM) curves of (a) Fe_3O_4, (b) Fe_3O_4@SiO_2, (c) Fe_3O_4@SiO_2@$(CH_2)_3Cl$, (d) Fe_3O_4@SiO_2@Im, (e) Fe_3O_4@SiO_2@Im-bisethylFc [Cl] and (f) Fe_3O_4@SiO_2@ Im-bisethylFc [HC_2O_4]

TABLE 2 Optimization of solvent, temperature, catalyst and amount of catalyst in the synthesis of bis-coumarin derivative **3a**

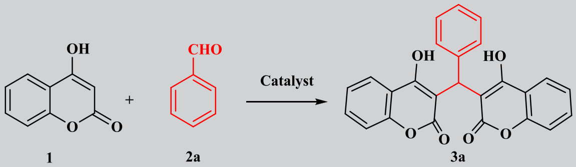

Entry	Catalyst	Catalyst amount (mg)	Solvent	Temperature (°C)	Time (hr)	Yield (%)
1	–	–	Free	80	7.3	9
2	Fe_3O_4	4	EtOH	Reflux	5	32
3	Fe_3O_4@SiO_2	4	EtOH	Reflux	5	23
4	Fe_3O_4@SiO_2@$(CH_2)_3Cl$	4	EtOH	Reflux	5	39
5	Fe_3O_4@SiO_2@Im	4	EtOH	Reflux	4	48
6	Fe_3O_4@SiO_2@Im-bisethylFc [Cl]	4	EtOH	Reflux	3	71
7	Fe_3O_4@SiO_2@Im-bisethylFc [HC_2O_4]	4	EtOH	Reflux	1	96
8	Fe_3O_4@SiO_2@Im-bisethylFc [HC_2O_4]	4	Free	80	3	56
9	Fe_3O_4@SiO_2@Im-bisethylFc [HC_2O_4]	4	EtOH:H_2O (50:50)	Reflux	2	88
10	Fe_3O_4@SiO_2@Im-bisethylFc [HC_2O_4]	4	MeOH	Reflux	2	91
11	Fe_3O_4@SiO_2@Im-bisethylFc [HC_2O_4]	4	CH_2Cl_2	Reflux	3	85
12	Fe_3O_4@SiO_2@Im-bisethylFc [HC_2O_4]	2	EtOH	Reflux	2.3	90
13	Fe_3O_4@SiO_2@Im-bisethylFc [HC_2O_4]	6	EtOH	Reflux	2	91

TABLE 3 The synthesis of new bis-coumarin derivatives in the presence of 4 mg $Fe_3O_4@SiO_2@Im$-bisethylFc $[HC_2O_4]$ under reflux in ethanol conditions

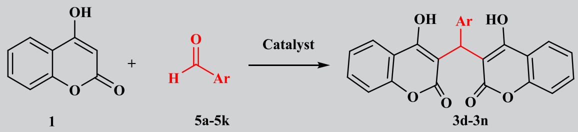

1 5a-5k 3d-3n

Catalyst : $Fe_3O_4@SiO_2@Im$-bisethylFc$[HC_2O_4]$

Entry	Aldehyde	Structure	Time (hr)	Yield (%)	Melting point (ºC)
1	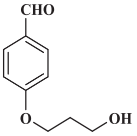 (5a)	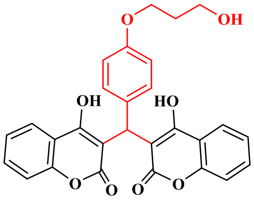 (3d)	4.30	88	185–188
2	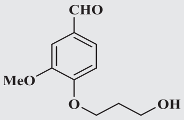 (5b)	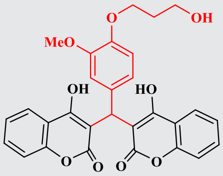 (3e)	5	84	160–162
3	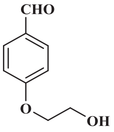 (5c)	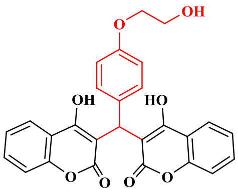 (3f)	4.30	87	188–190
4	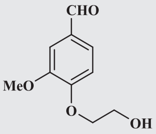 (5d)	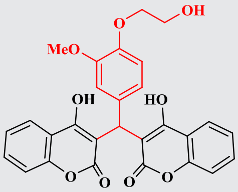 (3g)	5.15	84	150–152
5	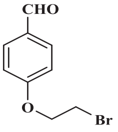 (5e)	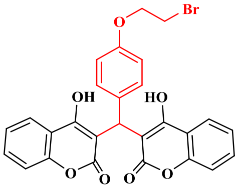 (3h)	4	90	273–275
6	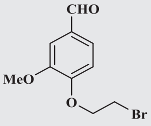 (5f)	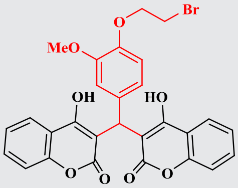 (3i)	4.15	89	125–127

(Continues)

TABLE 3 (Continued)

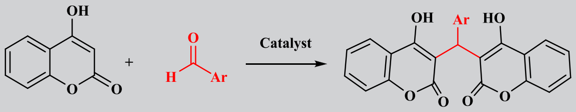

1 5a-5k 3d-3n

Catalyst : $Fe_3O_4@SiO_2@$Im-bisethylFc$[HC_2O_4]$

Entry	Aldehyde	Structure	Time (hr)	Yield (%)	Melting point (ºC)
7	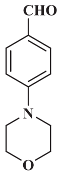 (5g)	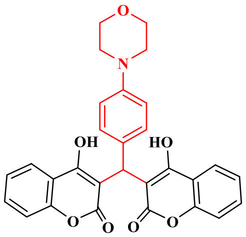 (3j)	4.45	85	206–208
8	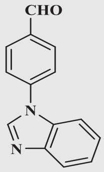 (5h)	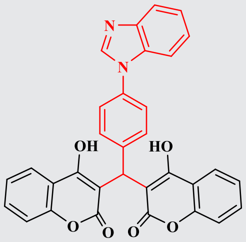 (3k)	3.30	91	308–310
9	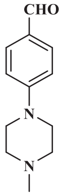 (5i)	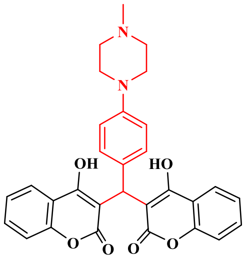 (3l)	4.45	85	222–224
10	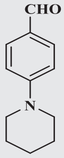 (5j)	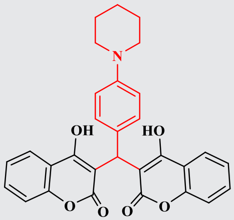 (3m)	4.45	86	170–172
11	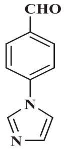 (5k)	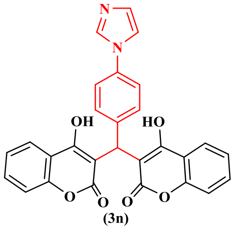 (3n)	3	93	267–269

The M-H loop behavior of all intermediates towards the desired catalyst is studied from VSM at room temperature (RT), varying the applied magnetic field (H) during the range of −10 000 to 10 000 Oe exhibit (Figure **7**). The saturation magnetizations (Ms) are found to be 58.88, 43.70, 34.7, 28.38, 20.8 and 18.63 emu/g for Fe_3O_4, $Fe_3O_4@SiO_2$, $Fe_3O_4@SiO_2@(CH_2)_3Cl$, $Fe_3O_4@SiO_2@Im$, $Fe_3O_4@SiO_2@Im$-bisethylFc [Cl] and $Fe_3O_4@SiO_2@$ Im-bisethylFc $[HC_2O_4]$, respectively. The synthesized nanoparticles exhibit superparamagnetic behavior. The value of saturation magnetization of all intermediates towards the desired catalyst has decreased compared with the pure Fe_3O_4. This difference suggests that silica and ferrocene-tagged IL is coated on the surface of Fe_3O_4 MNPs. In addition, we proved the magneticity of the synthesized nanocatalyst with an external magnet.

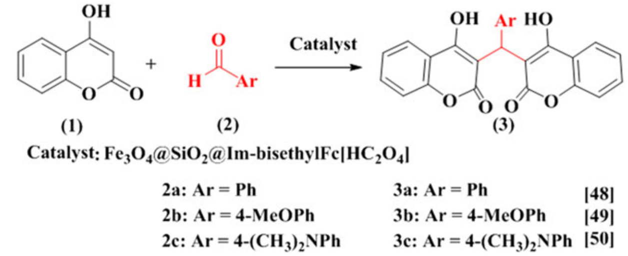

SCHEME 3 The synthesis of bis-coumarin derivatives in the presence of 4 mg Fe_3O_4@SiO_2@Im-bisFc [HC_2O_4] under reflux in ethanol conditions

2.2 | Application of Fe_3O_4@SiO_2@Im-bisethylFc [HC_2O_4] as a catalyst in the synthesis of bis-coumarin derivatives

In order to optimize the reaction conditions, the reaction of 4-hydroxycoumarin and benzaldehyde was chosen as a model reaction. Then we examined the reaction under various conditions, including different solvents, catalyst and temperatures, and also the use of different amounts of the synthesized nanocatalysts. The results are reported in Table 2, and the optimal conditions were obtained for reaction under reflux in ethanol and 4 mg of nanocatalyst for 1 mmol of benzaldehyde (Table 2, entry 7).

After improving the reaction conditions, we synthesized the bis-coumarin derivatives with different aromatic aldehydes under optimal conditions. According to the results reported in Table 3, bis-coumarin derivatives with aromatic aldehydes that have electron-withdrawing groups are synthesized over a short period of time and with high efficiency compared with

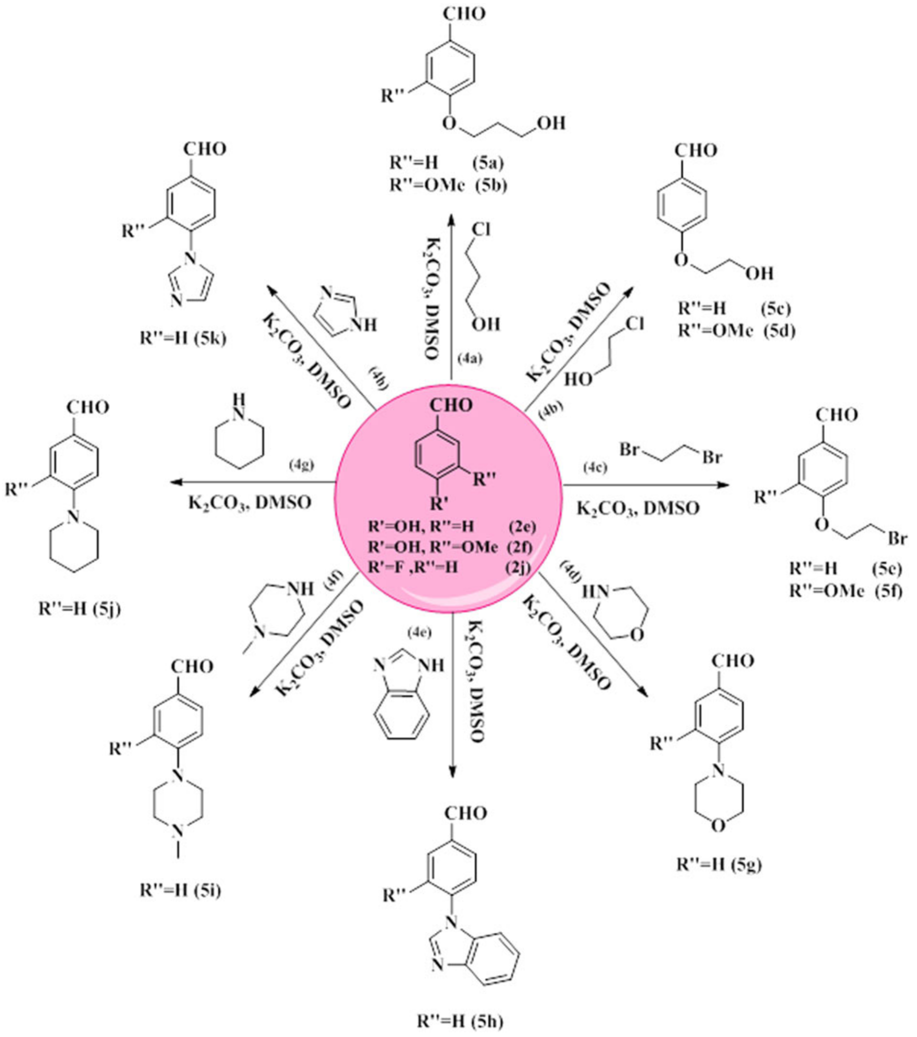

SCHEME 4 Synthesis of aromatic aldehyde derivatives (**5a–5k**)

aromatic aldehydes that have electron-donating groups (Scheme 3).

We also synthesized a series of aromatic aldehydes (Scheme **4**),[38–43] and applied them to synthesize new bis-coumarin derivatives using condensation of these aldehydes and 4-hydroxycoumarin catalyzed by Fe_3O_4@SiO_2@Im-bisethylFc [HC_2O_4] nanocatalyst under optimized conditions (Table 3)**.**

After synthesis of some novel bis-coumarin derivatives (**3d–3n**), in order to investigate the homoselectivity[48–51] of the synthesized nanocatalyst, we selected the reaction of terephthaldehyde (**5l**) as a dialdehyde derivative with 4-hydroxycoumarin in the presence of Im-bisethylFc [HC_2O_4] as a catalyst under optimized condition. Under similar conditions for the synthesis of bis-coumarin derivatives, in the reaction between 4-hydroxycoumarin (2 equiv.) and terephthaldehyde (1 equiv.), 3,3′-[(4-formylphenyl)methylene]bis(4-hydroxy-2*H*-chromen-2-one) (**3o**)[38] was obtained in 71% yield. By controlling the molar ratio of 4-hydroxycoumarin (4 equiv.) toward terephthaldehyde (1 equiv.), in this condensation reaction, 3,3′,3′′,3′′′-[1,4-phenylenebis (methanetriyl)] tetrakis(4-hydroxy-2*H*-chromen-2-one) (**3p**)[36] was gained in 82% yield (Scheme 5).

The Fe_3O_4@SiO_2@Im-bisethylFc [HC_2O_4] nanocatalyst has several Bronsted and Lewis acid and base sites, which can act as active sites of the nanocatalyst to promote this reaction (Figure 8). The Fe in the ferrocenyl unit of nanocatalyst can act as a Lewis acid.

The logical mechanism for the preparation of bis-coumarin derivatives by using Fe_3O_4@SiO_2@Im-bisethylFc [HC_2O_4] as catalyst is shown in Scheme 6. At first, 4-hydroxycoumarin reacts with the carbonyl group of the aldehyde, which is activated by Fe_3O_4@SiO_2@Im-bisethylFc [HC_2O_4] to produce the intermediate arylidenemalononitrile I. Then intermediate II was prepared by dehydration reaction from I. In the next step, the catalyst-activated 4-hydroxycoumarin undergoes a Michael-type addition reaction with II and, finally, the bis-coumarin derivative **3a** was produced.

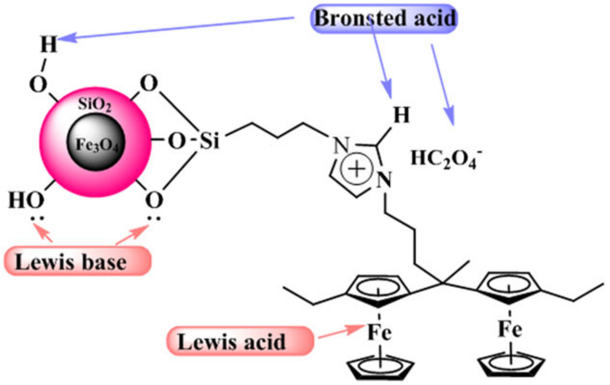

FIGURE 8 Various Bronsted and Lewis acid and base sites of Fe_3O_4@SiO_2@Im-bisethylFc [HC_2O_4] nanocatalyst

Finally, we investigated the reusability of the catalyst under reflux conditions in the presence of Fe_3O_4@SiO_2@Im-bisethylFc [HC_2O_4] nanocatalyst. After completion of the reaction, the catalyst was easily separated from the reaction mixture using external magnets. Subsequently, recycled magnetic nanocatalyst was washed with ethanol and dried in a vacuum. The recovered catalyst was reused for six runs (Figure 9).

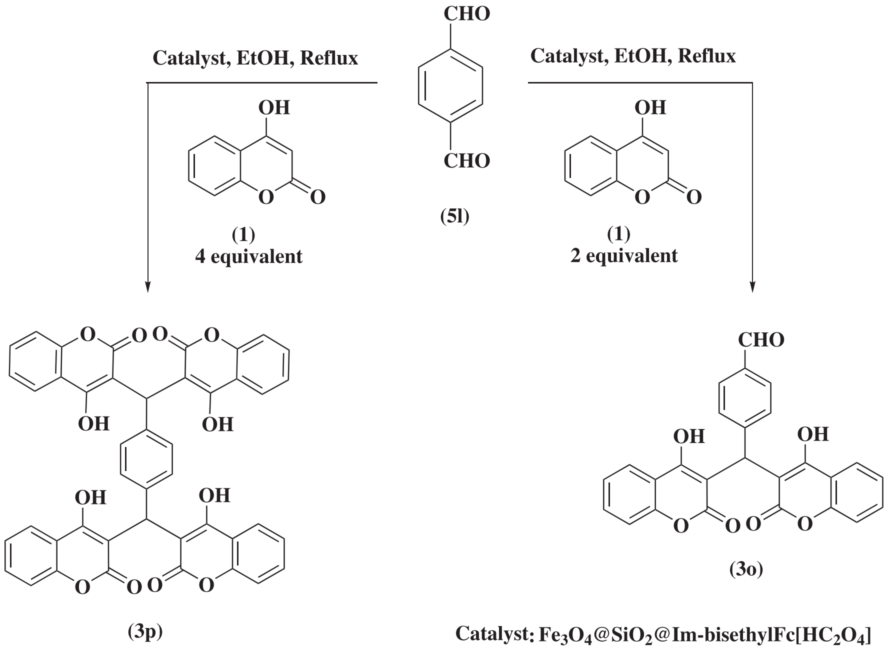

SCHEME 5 Investigation of the homoselectivity in the condensation reaction of 4-hydroxycoumarin with terephthaldehyde

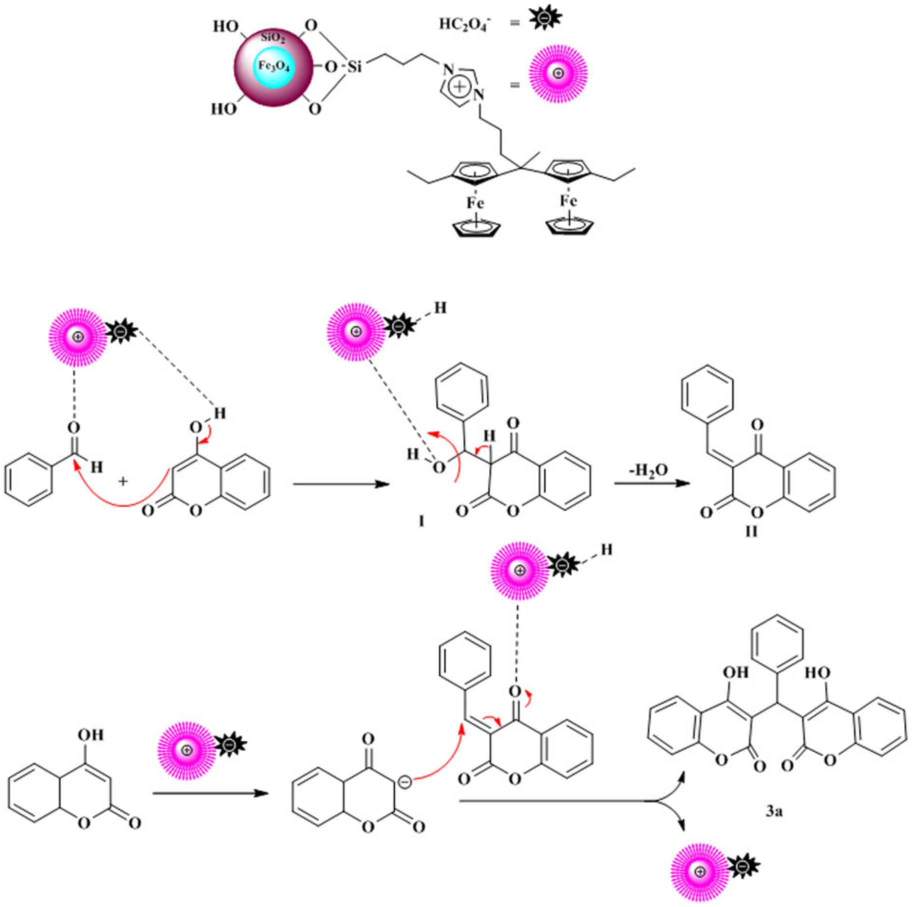

SCHEME 6 The logical mechanism for the synthesis of bis-coumarin derivative **3a** in the presence of $Fe_3O_4@SiO_2@$Im-bisethylFc [HC_2O_4] MNPs catalyst

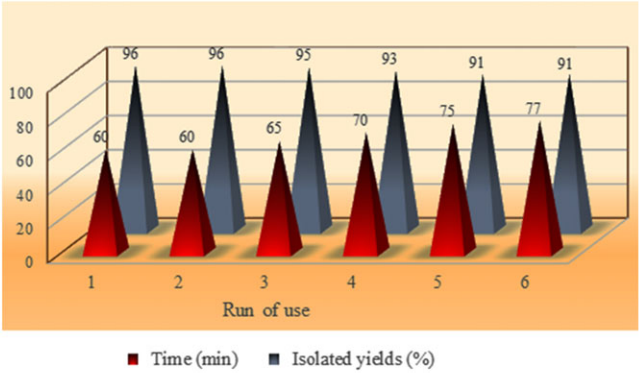

FIGURE 9 Reusability of $Fe_3O_4@SiO_2@$Im-bisethylFc [HC_2O_4] as a catalyst in the synthesis of bis-coumarin derivatives

The efficiency of the present method compared with a number of other reported works for the synthesis of bis-coumarin is summarized in Table 4. Although each of these methods has their own advantages, they suffer from some drawbacks, such as the use of long reaction times, low yield and use of non-recyclable catalyst. The present method offers a lot of advantages over most of the reported methods, such as, clean, simple and straightforward work-up, savings in energy consumption, a short reaction time and high yields.

3 | CONCLUSIONS

In this article, novel bisferrocenyl-based modified Fe_3O_4 MNPs were synthesized by using a facile co-preparation technique to investigate the catalytic application. The morphology and structure of the synthesized nanoparticles were characterized by a variety of methods, such as FT-IR spectroscopy, SEM and XRD techniques. Then the catalytic activity of the synthesized MNPs was investigated for the synthesis of some novel bis-coumarin derivatives. These MNPs exhibited good catalytic activity. Noteworthy advantages of this study are the relative simplicity of product isolation, cleaner reaction profiles, high yields, recyclability and reusability of the $Fe_3O_4@SiO_2@$Im-bisethylFc [HC_2O_4] catalyst.

TABLE 4 Comparison of results using $Fe_3O_4@SiO_2@$Im-bisethylFc $[HC_2O_4]$ MNPs with results obtained by other works for the synthesis of bis-coumarin

Entry	Catalyst	Conditions	Time (min)	Yield (%)	Ref.
1	[Pyridin-SO_3H]Cl	15 mol %; solvent-free/80°C	14	88	[36]
2	$[Fe_3O_4@SiO_2@(CH2)_3$-Im-$SO_3H]Cl$	7 mg; solvent-free/100°C	12	93	[37]
3	TrBr	15 mol%; solvent-free/100°C	20	92	[37]
4	MNPs-PSA	4.5 mg; solvent-free/RT	6	94	[38]
5	$Fe_3O_4@SiO_2@(CH_2)_3$semicarbazide-SO_3H/HCl	0.01 g; solvent-free/80°C	30	95	[39]
6	SiO_2Cl	75 mg; CH_2Cl_2/40°C	170	85	[52]
7	$[bmim]BF_4$	400 mol%; 60–70°C	120	84	[31]
8	Sodium dodecyl sulfate	20 mol%; water/60°C	150	90	[33]
9	IL [PSebim][OTf]	10 mol%; dried CH_2Cl_2/70°C	120	95	[32]
10	$Fe_3O_4@SiO_2@$Im-bisethylFc $[HC_2O_4]$	4 mg; EtOH/reflux	60	96	This work

RT, room temperature.

4 | EXPERIMENTAL

4.1 | General considerations

All chemicals were purchased from Merck or Aldrich chemical companies, and were used without further purification. Melting points were determined with a MEL-TEMP model 1202D and are uncorrected. FT-IR spectra were recorded on a Bruker Tensor 27 spectrometer as KBr disks. The ^{1}H-NMR spectra were recorded with a Bruker Spectrospin Avance 400 MHz spectrometer with $CDCl_3$ or DMSO-d_6 as solvent, and TMS as internal standard. ^{13}C-NMR spectra were determined on the same instrument at 100 MHz. All chemical shifts were reported as δ (ppm) relative to solvent peaks as internal standards, and coupling constants (J) are given in Hz. Elementary analyses were performed on a Vario EL III analyzer. XRD patterns of samples were taken on a Siemens D500 XRD diffractometer (CuK radiation, $\lambda = 1.5406$ A). EDX and FE-SEM images of the nanoparticles were visualized by a TESCAN MIRA3 FE-SEM. TEM images were obtained with a Zeiss EM 10C electron microscope. Magnetization measurement was carried out with a model 155 alternative gradient force magnetometer at RT.

4.2 | Synthesis of $Fe_3O_4@SiO_2@$Im-bisethylFc $[HC_2O_4]$ nanocatalyst

4.2.1 | Preparation of silica-coated Fe_3O_4 nanoparticles

Nanoparticles of Fe_3O_4 were produced by adding $FeCl_3{\cdot}6H_2O$ (5.4 g, 20 mmol) and $FeCl_2{\cdot}4H_2O$ (1.9 g, 10 mmol) to 200 mL water under nitrogen. Then, under rapid mechanical stirring, 2 M ammonia solution was added, and the pH value was controlled in the range $9 \leq pH \leq 12$. The mixture was stirred at 70°C for 15 min. The magnetite precipitate Fe_3O_4 was washed with distilled water and ethanol, and was dried under vacuum.

Two grams of Fe_3O_4 nanoparticles was dispersed in a mixture of 70 mL ethanol, 30 mL deionized water and 30 mL ammonia aqueous solution, followed by the addition of 4 mL tetraethyl orthosilicate (TEOS). The mixture was stirred with a mechanical stirrer for 24 hr. The modified nanoparticles ($Fe_3O_4@SiO_2$) were separated by a magnet from the reaction medium and washed with ethanol. The desired product was dried under vacuum.

4.2.2 | Preparation of $Fe_3O_4@SiO_2$-$(CH_2)_3Cl$ magnetic nanoparticles

Two grams of Fe_3O_4-silica-coated nanoparticles was added to 70 mL of dry toluene and placed in an ultrasonic bath for 30 min, then 3.18 mL of (3-chloropropyl) trimethoxysilane was added dropwise to the mixture. The mixture was stirred mechanically for 48 hr at 90°C. Modified nanoparticles $[Fe_3O_4@SiO_2$-$(CH_2)_3Cl]$ were separated by a magnet from the reaction medium, washed with ethanol and dried under vacuum.

4.2.3 | Preparation of $Fe_3O_4@SiO_2$-Imid magnetic nanoparticles

Two grams of $Fe_3O_4@SiO_2$-$(CH_2)_3Cl$ nanoparticles was added to 70 mL of dry toluene and placed in an ultrasonic bath for 30 min, then 1 g of imidazole and 4 mL of Et_3N was added to the mixture. The mixture was stirred mechanically for 24 hr at 95°C. Then, KI was added to the mixture and stirred mechanically for 24 hr. Modified nanoparticles ($Fe_3O_4@SiO_2$-Imid) were separated by a magnet from the reaction medium, washed with ethanol and dried under vacuum.

4.2.4 | Synthesis of 5-chloro-2,2-bis (ethylferrocenyl)pentane

At first, a mixture of dry methanol (5 mL) and sulfuric acid (50 mmol, 5.08 g) was mixed at RT under argon gas for 1 day. Then, the ethylferrocene (26 mmol, 5.58 g) was added to the mixture. After 20 min stirring, 5-chloro-2-pentanone (13 mmol, 1.5 mL) was added to the mixture at 60°C. The mixture was stirred for 10 hr at this temperature. Then the reaction mixture was cooled to RT and, after neutralization with sodium carbonate, was extracted with dichloromethane (3 × 25 mL). Then the solvent was removed by rotary evaporator and at the end the residue was purified by column chromatography. 5-Chloro-2,2-bis (ethylferrocenyl) pentane was obtained in 65% yield as orange oil with relatively high viscosity.[40]

4.2.5 | Synthesis of $Fe_3O_4@SiO_2@$Im-bisethylFc [cl]

Two grams of $Fe_3O_4@SiO_2$-Imid nanoparticles in 70 mL toluene was placed in the ultrasonic bath for 30 min. After fully dispersing of the nanoparticles, 1 g of 5-chloro-2,2-bis (ethylferrocenyl) pentane was added, and the reaction mixture was stirred with a mechanical stirrer at 90°C for 40 hr. Modified MNPs were separated from the reaction medium via an external magnetic field and washed with toluene. The desired product was dried under vacuum.

4.2.6 | Synthesis of $Fe_3O_4@SiO_2@$Im-bisethylFc [HC_2O_4]

At first, a mixture of oxalic acid dihydrate (2 mmol, 2.5 g) and sodium hydroxide (1 mmol, 0.4 g) in 40 mL of ethanol:water (30:10) was stirred at RT for 30 min. Then, 0.5 g of $Fe_3O_4@SiO_2@$Im-bisethylFc [Cl] nanoparticles was added and the mixture was put in the ultrasonic bath for 30 min. The suspension was stirred at RT for 48 hr by a mechanical stirrer. Modified nanoparticles were separated from the reaction medium via an external magnet, and washed with water and ethanol. The desired nanocatalyst was dried under vacuum. The modified nanoparticle was identified using FT-IR, FE-SEM, EDX, XRD, TEM and VSM analysis.

4.3 | General procedure for the synthesis of aldehyde derivatives

4.3.1 | Alkoxybenzaldehyde derivatives (5a–5d)

A mixture of benzaldehyde derivatives (1 mmol), compounds (3-chloropropanol or 2-chloroethanol; 1 mmol) and potassium carbonate (3 mmol) in dimethylsulfoxide was stirred for 8 hr. After completion of the reaction, which was monitored by thin-layer chromatography (TLC), the reaction mixture was diluted with water and extracted with dichloromethane. The solvent was removed under reduced pressure and the residue was purified through column chromatography.[53,54]

4.3.2 | Bromobenzaldehyde derivatives (5e, 5f)

Benzaldehyde derivatives (1 mmol) were dissolved in acetone (10 mL), then potassium carbonate (1 mmol) was added and the mixture was stirred for 24 hr under reflux. Then, 1,2-dibromoethane (10 mmol) and potassium carbonate (1 mmol) were added. The mixture was stirred for 72 hr under reflux and progress was controlled by TLC. After cooling to RT, water (20 mL) was added and the mixture was extracted with dichloromethane. The combined organic layers were washed with brine, dried over anhydrous sodium sulfate and the solvents were removed under reduced pressure. The residue was purified through column chromatography.[55,56]

4.3.3 | Aminobenzaldehyde derivatives (5g–5l)

A mixture of benzaldehyde derivatives (1 mmol), compounds (piperidine, 1-methylpiperazine, benzimidazole, morpholine and 1*H*-imidazole; 1 mmol) and potassium carbonate (1 mmol) in dimethylsulfoxide was refluxed for 24 hr. After completion of the reaction, which was monitored by TLC, the mixture was concentrated under low pressure and left to cool. The mixture was then poured into ice water and left overnight. The formed solid was filtered, washed with water and crystallized with methanol.[57,58]

4.4 | General procedure for the synthesis of bis-coumarin derivatives

A mixture of aromatic aldehyde (1 mmol), 4-hydroxycoumarin (2 mmol) and 4 mg of $Fe_3O_4@SiO_2@$Im-bisethylFc $[HC_2O_4]$ nanocatalyst in 30 mL of ethanol was stirred under reflux conditions for an appropriate time. After completion of the reaction follow by TLC (*n*-hexane:ethyl acetate; 3:7), the catalyst was separated from the reaction mixture by using an external magnet. The precipitate was filtered off and washed with ethanol, and the final pure product was obtained and characterized by FT-IR, ^{1}H-NMR, ^{13}C-NMR and CHNS analyses. The characterization data for the synthesized compounds are given below. Also, the NMR spectra are given in the Supporting Information.

4.4.1 | 3,3′-[(4-Methoxyphenyl)methylene]bis(4-hydroxy-2*H*-chromen-2-one) (3b)

White solid; yield: 88%; m.p. 154–156°C. ^{1}H-NMR (400 MHz, DMSO-d_6): δ 3.70 (3H, s, OCH_3), 6.28 (1H, s, CH), 6.79 (2H, d, $J = 12$ Hz, Ar-H), 7.06 (2H, d, $J = 8$ Hz, Ar-H), 7.31–7.38 (4H, m, Ar-H), 7.60 (2H, t, $J = 8$ Hz, Ar-H), 7.90 (2H, d, $J = 8$ Hz, Ar-H) ppm; anal. calcd for $C_{20}H_{14}O_7$: C, 65.58%; H, 3.85%; found: C, 65.38%; H, 3.90%.

4.4.2 | 3,3′-[(4-Dimethylaminophenyl)methylene]bis(4-hydroxy-2*H*-chromen-2-one) (3c)

White solid; yield: 85%; m.p. 210–212°C. ^{1}H-NMR (400 MHz, DMSO-d_6): δ 3.13 (6H, s, N $(CH_3)_2$), 6.28 (1H, s, CH), 7.21–7.28 (6H, m, Ar-H), 7.41 (2H, d, $J = 12$ Hz, Ar-H), 7.51 (2H, t, $J = 8$ Hz, Ar-H), 7.81 (2H, d, $J = 8$ Hz, Ar-H) ppm; anal. calcd for $C_{21}H_{17}NO_6$: C, 71.20%; H, 4.65%; N, 3.08%; found: C, 70.90%; H, 4.70%; N, 3.00%.

4.4.3 | 3,3′-[(4-(3-Hydroxypropoxy)phenyl)methylene]bis(4-hydroxy-2*H*-chromen-2-one) (3d)

White solid; yield: 88%; m.p. 185–188°C. FT-IR (KBr) ν 1089, 1463, 1619, 1671, 2929, 3058, 3443 cm^{-1}; ^{1}H-NMR (400 MHz, DMSO-d_6): δ 1.79–1.85 (2H, m, CH_2), 3.51–3.57 (2H, m, CH_2-OH), 3.95–3.98 (2H, m, PhO-CH_2), 4.72 (3H, br, OH), 6.28 (1H, s, CH), 6.80 (2H, d, $J = 8$ Hz, Ar-H), 7.05 (2H, d, $J = 8$ Hz, Ar-H), 7.32–7.39 (4H, m, Ar-H), 7.61 (2H, d, $J = 8$ Hz, Ar-H), 7.91 (2H, t, $J = 8$ Hz, Ar-H) ppm. ^{13}C-NMR (100 MHz, DMSO-d_6): δ 32.20, 35.29, 57.31, 64.46, 104.47, 114.11, 116.08, 117.55, 123.87, 123.96, 127.82, 130.88, 132.12, 152.16, 156.90, 164.64, 164.87 ppm; anal. calcd for $C_{28}H_{22}O_8$: C, 69.13%; H, 4.56%; found: C, 68.93%; H, 4.61%.

4.4.4 | 3,3′-[(4-(3-Hydroxypropoxy)-3-methoxyphenyl)methylene]bis(4-hydroxy-2*H*-chromen-2-one) (3e)

White solid; yield: 84%; m.p. 160–162°C. FT-IR (KBr) ν 1097, 1458, 1613, 1663, 2930, 3074, 3435 cm^{-1}. ^{1}H-NMR (400 MHz, DMSO-d_6): δ 1.81–1.84 (2H, m, CH_2), 3.51–3.56 (5H, m, CH_2-OH, OCH_3), 3.95 (2H, t, $J = 6$ Hz, PhO-CH_2), 4.12 (3H, s, OH), 6.26 (1H, s, CH), 6.65 (1H, d, $J = 8$ Hz, Ar-H), 6.71 (1H, s, Ar-H), 6.80 (1H, d, $J = 8$ Hz, Ar-H), 7.30–7.37 (4H, m, Ar-H), 7.59 (2H, t, $J = 8$ Hz, Ar-H), 7.90 (2H, d, $J = 8$ Hz, Ar-H) ppm. ^{13}C-NMR (100 MHz, DMSO-d_6): δ 32.26, 35.67, 55.72, 57.42, 65.35, 104.34, 111.68, 112.77, 115.96, 117.91, 118.97, 123.75, 123.86, 131.86, 132.18, 146.52, 148.74, 152.19, 164.71, 165.04 ppm; anal. calcd for $C_{29}H_{24}O_9$: C, 67.44%; H, 4.68%; found: C, 67.22%; H, 4.72%.

4.4.5 | 3,3′-[(4-(2-Hydroxyethoxy)phenyl)methylene]bis(4-hydroxy-2*H*-chromen-2-one) (3f)

White solid; yield: 87%; m.p. 188–190°C. FT-IR (KBr) ν 1091, 1453, 1614, 1664, 2930, 3074, 3434 cm^{-1}. ^{1}H-NMR (400 MHz, DMSO-d_6): δ 3.68 (2H, t, $J = 6$ Hz, CH_2-OH), 3.92 (2H, t, $J = 6$ Hz, PhO-CH_2), 4.73 (3H, br, OH), 6.29 (1H, s, CH), 6.81 (2H, d, $J = 12$ Hz, Ar-H), 6.05 (2H, d, $J = 8$ Hz, Ar-H), 7.32–7.39 (4H, m, Ar-H), 7.61 (2H, t, $J = 8$ Hz, Ar-H), 7.91 (2H, d, $J = 8$ Hz, Ar-H) ppm. ^{13}C-NMR (100 MHz, DMSO-d_6): δ 35.27, 59.58, 69.40, 104.44, 114.13, 116.04, 117.61, 123.86, 123.90, 127.80, 131.05, 132.05, 152.16, 156.84, 164.72, 165.84 ppm; anal. calcd for $C_{27}H_{20}O_8$: C, 68.64%; H, 4.27%; found: C, 68.51%; H, 4.32%.

4.4.6 | 3,3′-[(4-(2-Hydroxyethoxy)-3-methoxyphenyl)methylene]bis(4-hydroxy-2*H*-chromen-2-one) (3g)

White solid; yield: 84%; m.p. 150–152°C. FT-IR (KBr) ν 1095, 1455, 1614, 1662, 2929, 3075, 3434 cm^{-1}. ^{1}H-NMR (400 MHz, DMSO-d_6): δ 3.56 (3H, s, OCH_3), 3.68 (2H, t, $J = 8$ Hz, CH_2-OH), 3.90 (2H, t, $J = 8$ Hz, PhO-CH_2), 5.75 (3H, br, OH), 6.26 (1H, s, CH), 6.64 (1H, d, $J = 8$ Hz, Ar-H), 6.72 (1H, s, Ar-H), 6.81 (1H, d, $J = 8$ Hz, Ar-H), 7.30–7.36 (4H, m, Ar-H), 7.58 (2H, t, $J = 8$ Hz, Ar-

H), 7.89 (2H, d, $J = 8$ Hz, Ar-H) ppm. ^{13}C-NMR (100 MHz, DMSO-d_6): δ 35.68, 55.55, 59.63, 70.16, 104.33, 111.43, 112.82, 115.98, 118.15, 118.89, 123.73, 123.93, 131.83, 132.56, 146.39, 148.69, 152.25, 164.76, 165.40 ppm; anal. calcd for $C_{28}H_{22}O_9$: C, 66.93%; H, 4.41%; found: C, 66.70%; H, 4.50%.

4.4.7 | 3,3′-[(4-(2-Bromoethoxy)phenyl)methylene]bis(4-hydroxy-2*H*-chromen-2-one) (3h)

Yellow solid; yield: 90%; m.p. 273–275°C. FT-IR (KBr) ν 458, 1085, 1450, 1609, 1667, 2927, 3066, 3434 cm^{-1}. ^{1}H-NMR (400 MHz, DMSO-d_6): δ 4.01–4.03 (2H, m, CH$_2$-Br), 4.23 (2H, br, PhO-CH$_2$), 6.28 (1H, s, CH), 6.82 (2H, d, $J = 12$ Hz, Ar-H), 7.06 (2H, d, $J = 8$ Hz, Ar-H), 7.30–7.37 (4H, m, Ar-H), 7.59 (2H, t, $J = 8$ Hz, Ar-H), 7.88 (2H, d, $J = 8$ Hz, Ar-H), ppm. ^{13}C-NMR (100 MHz, DMSO-d_6): δ 31.57, 35.27, 66.32, 104.34, 114.11, 115.92, 117.86, 123.72, 123.85, 127.80, 131.69, 131.85, 152.16, 156.43, 164.77, 165.06 ppm; anal. calcd for $C_{27}H_{19}BrO_7$: C, 60.58%; H, 3.58%; found: C, 60.28%; H, 3.62%.

4.4.8 | 3,3′-[(4-(2-Bromoethoxy)-3-methoxyphenyl)methylene]bis(4-hydroxy-2*H*-chromen-2-one) (3i)

Yellow solid; yield: 89%; m.p. 125–127°C. FT-IR (KBr) ν 458, 1096, 1457, 1644, 1658, 2925, 3062, 3453 cm^{-1}. ^{1}H-NMR (400 MHz, DMSO-d_6): δ 3.57 (3H, s, OCH$_3$), 3.75 (2H, t, $J = 8$ Hz, CH$_2$-Br), 3.90 (2H, br, OH), 4.22 (2H, t, $J = 8$ Hz, PhO-CH$_2$), 6.24 (1H, s, CH), 6.64 (1H, d, $J = 8$ Hz, Ar-H), 6.72 (1H, s, Ar-H), 6.81 (1H, d, $J = 8$ Hz, Ar-H), 7.26–7.32 (4H, m, Ar-H), 7.55 (2H, t, $J = 8$ Hz, Ar-H), 7.86 (2H, d, $J = 8$ Hz, Ar-H) ppm. ^{13}C-NMR (100 MHz, DMSO-d_6): δ 31.57, 35.71, 55.78, 68.83, 104.03, 111.98, 113.90, 115.77, 118.73, 119.04, 123.41, 123.96, 131.48, 134.45, 145.43, 148.82, 152.31, 164.64, 166.18 ppm; anal. calcd for $C_{28}H_{21}BrO_8$: C, 59.48%; H, 3.74%; found: C, 59.28%; H, 3.84%.

4.4.9 | 3,3′-[(4-(Morpholin-4-yl)phenyl)methylene]bis(4-hydroxy-2*H*-chromen-2-one) (3j)

Pink solid; yield: 85%; m.p. 206–208°C. FT-IR (KBr) ν 1077, 1304, 1447, 1613, 1670, 2960, 3043, 3424 cm^{-1}. ^{1}H-NMR (400 MHz, DMSO-d_6): δ 3.42 (4H, s, N (CH$_2$)$_2$), 3.87 (4H, s, O (CH$_2$)$_2$), 6.29 (1H, s, CH), 7.18–7.31 (8H, m, Ar-H), 7.54 (2H, t, $J = 8$ Hz, Ar-H), 7.84 (2H, d, $J = 8$ Hz, Ar-H) ppm. ^{13}C-NMR (100 MHz, DMSO-d_6): δ 35.69, 52.28, 64.76, 103.48, 115.69, 118.58, 119.01, 123.26, 124.01, 127.93, 131.39, 152.39, 164.57, 166.69 ppm; anal. calcd for $C_{29}H_{23}NO_7$: C, 70.01%; H, 4.66%; N, 2.82%; found: C, 69.81%; H, 4.76%; N, 2.75%.

4.4.10 | 3,3′-[(4-(1*H*-benzo [d]imidazol-1-yl)phenyl)methylene]bis(4-hydroxy-2*H*-chromen-2-one) (3k)

Pink solid; yield: 91%; m.p. 267–269°C. FT-IR (KBr) ν 1031, 1329, 1408, 1609, 1673, 2909, 3159, 3430 cm^{-1}. ^{1}H-NMR (400 MHz, DMSO-d_6): δ 4.25 (2H, br, OH), 6.41 (1H, s, CH), 7.23–7.30 (4H, m, Ar-H), 7.42 (2H, d, $J = 8$ Hz, Ar-H), 7.51–7.63 (7H, m, Ar-H), 7.77 (2H, d, Ar-H), 7.84 (2H, d, $J = 8$ Hz, Ar-H), 7.92 (1H, d, $J = 8$ Hz, Ar-H(, 9.07 (1H, s, N-CH=N) ppm. ^{13}C-NMR (100 MHz, DMSO-d_6): δ 36.17, 103.05, 112.87, 115.57, 115.79, 119.68, 123.00, 124.12, 124.32, 126.08, 126.28, 130.84, 131.15, 152.54, 164.46, 167.71 ppm; anal. calcd for $C_{32}H_{20}N_2O_6$: C, 72.72%; H, 3.81%; N, 5.30%; found: C, 72.62%; H, 3.90%; N, 5.21%.

4.4.11 | 3,3′-[(4-(4-Methylpiperazin-1-yl)phenyl)methylene]bis(4-hydroxy-2*H*-chromen-2-one) (3l)

Pink solid; yield: 85%; m.p. 222–224°C. FT-IR (KBr) ν 1036, 1340, 1400, 1607, 1664, 2939, 3054, 3450 cm^{-1}. ^{1}H-NMR (400 MHz, DMSO-d_6): δ 2.83 (3H, s, CH$_3$), 3.35 (8H, m, 4CH$_2$), 3.84 (2H, br, OH), 6.19 (1H, s, CH), 6.81 (2H, d, $J = 8$ Hz, Ar-H), 6.98 (2H, d, $J = 8$ Hz, Ar-H), 7.19–7.26 (4H, m, Ar-H), 7.49 (2H, d, $J = 8$ Hz, Ar-H), 7.79 (2H, d, $J = 8$ Hz, Ar-H) ppm. ^{13}C-NMR (100 MHz, DMSO-d_6): δ 35.33, 42.10, 46.23, 52.45, 103.54, 115.43, 115.83, 119.94, 122.82, 124.04, 127.37, 130.82, 134.31, 146.94, 152.46, 164.52, 167.55 ppm; anal. calcd for $C_{30}H_{26}N_2O_6$: C, 70.58%; H, 5.13%; N, 5.49%; found: C, 70.35%; H, 5.23%; N, 5.40%.

4.4.12 | 3,3′-[(4-(Piperidin-1-yl)phenyl)methylene]bis(4-hydroxy-2*H*-chromen-2-one) (3m)

Pink solid; yield: 86%; m.p. 170–172°C. FT-IR (KBr) ν 1027, 1329, 1402, 1612, 1673, 2937, 3054, 3424 cm^{-1}. ^{1}H-NMR (400 MHz, DMSO-d_6): δ 1.62 (2H, br, CH$_2$), 1.85 (4H, br, 2CH$_2$), 3.43–3.56 (6H, m, OH and 2CH$_2$), 6.30 (1H, s, CH), 7.21–7.28 (6H, m, Ar-H), 7.48–7.53 (4H, m, Ar-H), 7.80 (2H, d, $J = 8$ Hz, Ar-H) ppm. ^{13}C-NMR (100 MHz, DMSO-d_6): δ 20.66, 23.44, 36.00, 56.01, 102.94, 115.56, 119.74, 120.61, 123.00, 124.13, 128.22, 131.14, 152.54, 164.45, 167.76 ppm; anal. calcd for $C_{30}H_{25}NO_6$: C, 72.72%; H, 5.09%; N, 2.83%; found: C, 72.55%; H, 5.18%; N, 2.78%.

4.4.13 | 3,3′-[(4-(1*H*-Imidazol-1-yl)phenyl) methylene]bis(4-hydroxy-2*H*-chromen-2-one) (3n)

Pink solid; yield: 93%; m.p. 308–310°C. FT-IR (KBr) ν 1043, 1326, 1400, 1610, 1685, 2913, 3148, 3445 cm^{-1}. ^1H-NMR (400 MHz, DMSO-d_6): δ 3.40 (2H, br s, OH), 6.33 (1H, s, CH), 7.21–7.32 (6H, m, Ar-H), 7.50–7.57 (4H, m, Ar-H), 7.79–7.86 (3H, m, Ar-H), 8.20 (1H, s, CH-N), 9.56 (1H, s, CH-N) ppm. ^{13}C-NMR (100 MHz, DMSO-d_6): δ 106.56, 110.78, 111.97, 112.10, 112.70, 113.97, 115.10, 119.13, 122.09, 123.20, 125.44, 135.42, 143.54, 155.40, 158.79 ppm; anal. calcd for $C_{28}H_{18}N_2O_6$: C, 70.29%; H, 3.79%; N, 5.86%; found: C, 70.08%; H, 3.85%; N, 5.80%.

ACKNOWLEDGEMENT

The authors thank research affairs of the University of Tabriz for financial support.

ORCID

Reza Teimuri-Mofrad https://orcid.org/0000-0002-5812-6445

REFERENCES

[1] L. Han, S. W. Park, D. W. Park, *Energy Environ. Sci.* **2009**, *2*, 1286.

[2] R. N. Baig, R. S. Varma, *Chem. Commun.* **2013**, *49*, 752.

[3] J. Safari, Z. Zarnegar, *C. R. Chim.* **2013**, *16*, 920.

[4] P. Wasserscheid, T. Welton, *Ionic liquids in synthesis* 2nd edn, Weinheim, Germany, **2008**.

[5] C. Yue, D. Fang, L. Liu, T. F. Yi, *J. Mol. Liq.* **2011**, *163*, 99.

[6] J. Dupont, R. F. de Souza, P. A. Suarez, *Chem. Rev.* **2002**, *102*, 3667.

[7] J. Suresh, S. Sandhu, *Green Chem. Lett. Rev.* **2011**, *4*, 311.

[8] M. N. Shaikh, M. A. Aziz, A. Helal, M. Bououdina, Z. H. Yamani, T. J. Kim, *RSC Adv.* **2016**, *6*, 41 687.

[9] J. Liu, S. Tian, L. Tiefenauer, P. E. Nielsen, W. Knoll, *Anal. Chem.* **2005**, *77*, 2756.

[10] M. Esmaeilpour, J. Javidi, F. NowrooziDodeji, M. MokhtariAbarghoui, *Transition Met. Chem.* **2014**, *39*, 797.

[11] A. N. Kozitsina, N. N. Malysheva, I. A. Utepova, Y. A. Glazyrina, A. I. Matern, K. Z. Brainina, O. N. Chupakhin, *J. Anal. Chem.* **2015**, *70*, 540.

[12] H. Zhao, N. Neamati, H. Hong, A. Mazumder, S. Wang, S. Sunder, G. W. A. Milne, Y. Pommier, T. R. Burke, *J. Med. Chem.* **1997**, *40*, 242.

[13] M. I. Choudhary, N. Fatima, K. M. Khan, S. Jalil, S. Iqbal, *Bioorg. Med. Chem.* **2006**, *14*, 8066.

[14] I. Manolov, C. Maichle-Moessmer, N. Danchev, *Eur. J. Med. Chem.* **2006**, *41*, 882.

[15] G. Appendino, G. Cravotto, S. Tagliapietra, S. Ferraro, G. M. Nano, G. Palmisano, *Helv. Chim. Acta* **1991**, *74*, 1451.

[16] A. Sahar, Z. A. Khan, M. Ahmad, A. F. Zahoor, A. Mansha, A. Iqbal, *Trop. J. Pharm. Res.* **2017**, *16*, 203.

[17] V. D. Kancheva, P. V. Boranova, J. T. Nechev, I. I. Manolov, *Biochimie* **2010**, *92*, 1138.

[18] J. Li, Y. P. Sui, J. J. Xin, X. L. Du, J. T. Li, H. R. Huo, H. Ma, W. H. Wang, H. Y. Zhou, H. D. Zhan, Z. J. Wang, C. Li, F. Sui, X. Li, *Bioorg. Med. Chem. Lett.* **2015**, *25*, 5520.

[19] K. M. Khan, F. Rahim, A. Wadood, N. Kosar, M. Taha, S. Lalani, A. Khan, M. I. Fakhri, M. Junaid, W. Rehman, M. Khan, S. Perveen, M. Sajid, M. I. Choudhary, *Eur. J. Med. Chem.* **2014**, *81*, 245.

[20] K. M. Khan, S. Iqbal, M. A. Lodhi, G. M. Maharvi, M. I. Choudhary, S. Perveen, *Bioorg. Med. Chem.* **2004**, *12*, 1963.

[21] K. M. Khan, A. Wadood, M. Ali, Z. Ul-Haq, Z. Ul-Haq, M. A. Lodhi, M. Khan, M. Khan, S. Perveen, M. I. Choudhary, *J. Mol. Graphics Modell.* **2010**, *28*, 792.

[22] O. Talhi, M. Schnekenburger, J. Panning, D. G. Pinto, J. A. Fernandes, F. A. A. Paz, C. Jacob, M. Diederich, A. M. Silva, *Bioorg. Med. Chem.* **2014**, *22*, 3008.

[23] J. Li, X. Y. Xue, X. Li, Z. Hou, X. H. Yang, D. Qu, Y. Zhou, Z. D. Zhang, X. X. Luo, J. T. Li, M. K. Li, *Arch. Pharmacol. Res.* **2016**, *39*, 1349.

[24] J. Xu, J. Ai, S. Liu, X. Peng, L. Yu, M. Geng, F. Nan, *Org. Biomol. Chem.* **2014**, *12*, 3721.

[25] N. Hamdi, M. C. Puerta, P. Valerga, *Eur. J. Med. Chem.* **2008**, *43*, 2541.

[26] D. Završnik, S. Muratović, D. Makuc, J. Plavec, M. Cetina, A. Nagl, E. De Clercq, J. Balzarini, M. Mintas, *Molecules* **2011**, *16*, 6023.

[27] M. Faisal, A. Saeed, D. Shahzad, T. A. Fattah, B. Lal, P. A. Channar, J. Mahar, S. Saeed, P. A. Mahesar, F. A. Larik, *Eur. J. Med. Chem.* **2017**, *141*, 386.

[28] C. X. Su, J. F. Mouscadet, C. C. Chiang, H. J. Tsai, L. Y. Hsu, *Chem. Pharm. Bull.* **2006**, *54*, 682.

[29] J. M. Khurana, S. Kumar, *Tetrahedron Lett.* **2009**, *50*, 4125.

[30] M. Kidwai, V. Bansal, P. Mothsra, S. Saxena, R. K. Somvanshi, S. Dey, T. P. J. Singh, *Mol. Catal. A: Chem.* **2007**, *268*, 76.

[31] J. M. Khurana, S. Kumar, *Monatsh. Chem.* **2010**, *141*, 561.

[32] W. Li, Y. Wang, Z. Wang, L. Dai, Y. Wang, *Catal. Lett.* **2011**, *141*, 1651.

[33] H. Mehrabi, H. Abusaidi, *J. Iran. Chem. Soc.* **2010**, *7*, 890.

[34] J. Li, Z. Hou, G. H. Chen, F. Li, Y. Zhou, X. Y. Xue, Z. P. Li, M. Jia, Z. D. Zhang, M. K. Li, X. X. Luo, *Org. Biomol. Chem.* **2014**, *12*, 5528.

[35] B. Pawar, V. Shinde, A. Chaskar, *Green Sustain Chem.* **2013**, *3*, 56.

[36] M. A. Zolfigol, A. R. Moosavi-Zare, M. Zarei, *C. R. Chim.* **2014**, *17*, 1264.

[37] M. Zarei, M. A. Zolfigol, A. R. Moosavi-Zare, E. Noroozizadeh, *J. Iran. Chem. Soc.* **2017**, *14*, 2187.

[38] H. Ghasemnejad-Bosra, A. Rostami, *Iran. Chem. Commun.* **2017**, *5*, 129.

[39] M. A. Zolfigol, R. Ayazi-Nasrabadi, S. Baghery, *Appl. Organomet. Chem.* **2016**, *30*, 500.

[40] R. Teimuri-Mofrad, S. Esmati, S. Tahmasebi, M. Gholamhosseini-Nazari, *J. Organomet. Chem.* **2018**, *870*, 38.

[41] R. Teimuri-Mofrad, M. Gholamhosseini-Nazari, E. Payami, S. Esmati, *Res. Chem. Intermed.* **2017**, *43*, 7105.

[42] R. Teimuri-Mofrad, M. Gholamhosseini-Nazari, E. Payami, S. Esmati, *Appl. Organomet. Chem.* **2018**, *32*, 3955.

[43] R. Teimuri-Mofrad, S. Esmati, M. Rabiei, M. Gholamhosseini-Nazari, *Heterocycl. Commun.* **2017**, *23*, 439.

[44] R. Teimuri-Mofrad, S. Esmati, M. Rabiei, M. Gholamhosseini-Nazari, *J. Chem. Res.* **2018**, *42*, 7.

[45] W. Stöber, A. Fink, E. Bohn, *J. Colloid Interface Sci.* **1968**, *26*, 62.

[46] K. Nishio, M. Ikeda, N. Gokon, S. Tsubouchi, H. Narimatsu, Y. Mochizuki, S. Sakamoto, A. Sandhu, M. Ab, H. Handa, *J. Magn. Magn. Mater.* **2007**, *310*, 2408.

[47] Y. Deng, D. Qi, C. Deng, X. Zhang, D. Zhao, *J. Am. Chem. Soc.* **2008**, *130*, 28.

[48] (a) M. A. Zolfigol, F. Shirini, A. G. Choghamarani, *Synthesis* **2006**, *12*, 2043. (b) M. A. Zolfigol, K. Amani, A. Ghorbani-Choghamarani, M. Hajjami, R. Ayazi-Nasrabadi, S. Jafari, *Catal. Commun.* **2008**, *9*, 1739. (c) K. Amani, M. A. Zolfigol, A. Ghorbani-Choghamarani, M. Hajjami, *Monatsh. Chem.* **2009**, *140*, 65. (d) G. Chehardoli, M. A. Zolfigol, *Phosphorus Sulfur Silicon* **2010**, *185*, 193. (e) A. Hasaninejad, G. Chehardoli, M. A. Zolfigol, A. Abdoli, *Phosphorus Sulfur Silicon* **2011**, *186*, 271.

[49] R. Karimian, F. Piri, A. A. Safari, S. J. Davarpanah, *J. Nanostructure Chem* **2013**, *3*, 52.

[50] C. Sirichaiwat, C. Intaraudom, S. Kamchonwongpaisan, J. Vanichtanankul, Y. Thebtaranonth, Y. Yuthavong, *J. Med. Chem.* **2004**, *47*, 345.

[51] Y. L. Zhao, L. Hu, G. Grüner, J. F. Stoddart, *J. Am. Ceram. Soc.* **2008**, *130*, 16 996.

[52] C. P. Ortmeyer, G. Haufe, K. Schwegmann, S. Hermann, M. Schaefers, F. Börgel, V. Hugenberg, *Bioorg. Med. Chem.* **2017**, *25*, 2167.

[53] N. Senthilkumar, Y. S. Somannavar, S. B. Reddy, B. K. Sinha, G. K. A. S. S. Narayan, R. Dandala, K. Mukkanti, *Synth. Commun.* **2010**, *41*, 268.

[54] P. Magdolen, M. Mečiarová, Š. Toma, *Tetrahedron* **2001**, *57*, 4781.

[55] M. M. Abdel-Atty, N. A. Farag, S. E. Kassab, R. A. Serya, K. A. Abouzid, *Bioorg. Chem.* **2014**, *57*, 65.

[56] V. D. Patil, K. P. Patil, N. R. Sutar, P. V. Gidh, *Chem. Int.* **2017**, *3*, 240.

[57] H. Y. Zhou, F. Q. Dong, X. L. Du, Z. K. Zhou, H. R. Huo, W. H. Wang, H. D. Zhan, Y. F. Dai, J. Meng, Y. P. Sui, J. Li, F. Sui, Y. H. Zhai, *Bioorg. Med. Chem. Lett.* **2016**, *26*, 3876.

[58] D. Završnik, S. Muratović, S. Špirtović, D. Softić, M. Medić-Šarić, *Bosnian J. Basic. Med. Sci.* **2008**, *8*, 277.

SUPPORTING INFORMATION

Additional supporting information may be found online in the Supporting Information section at the end of the article.

How to cite this article: Teimuri-Mofrad R, Tahmasebi S, Payami E. Fe_3O_4@SiO_2@Im-bisethylFc [HC_2O_4] as a novel recyclable heterogeneous nanocatalyst for synthesis of bis-coumarin derivatives. *Appl Organometal Chem*. 2019;e4773. https://doi.org/10.1002/aoc.4773